

---

## **Prestress evaluation in prestressed concrete plate-like structures**

---

Thisara S. Pathirage\*, Tommy H.T. Chan,  
David P. Thambiratnam and Andy Nguyen

Faculty of Science and Engineering,  
School of Civil Engineering and Built Environment,  
Queensland University of Technology,  
Brisbane, Australia  
Email: thisara.pathirage@qut.edu.au  
Email: tommy.chan@qut.edu.au  
Email: d.thambiratnam@qut.edu.au  
Email: a68.nguyen@qut.edu.au  
\*Corresponding author

**H.N.P. Moragaspitiya**

K and K Consulting Engineers Pty Ltd,  
11/30 Lindeman Place,  
Eight Miles Planes,  
QLD 4113, Brisbane, Australia  
Email: kandkce@gmail.com

**Abstract:** Condition assessment and capacity evaluation of existing structures using their vibration responses have been subjected to extensive research for many years. Prestressed concrete structures have been one of the main focuses of those studies. In the case of prestressed concrete structures, effective prestress force is the most important parameter for their best performance and yet currently there is no effective method for identifying the prestressing force in an existing prestressed concrete structure. Effect of prestressing is different for different types of structural elements and has to be treated accordingly for its accurate quantification. This paper presents a new approach to evaluate the effective prestress force of plate-like structures with simply supported boundary conditions using their vibration responses. The proposed method quantifies the prestress effect with a reasonable good accuracy, even with noisy measurements using both periodic and impulsive excitations. Prestress estimation can be done using collected data from as less as two measurement locations.

**Keywords:** effective prestress force; plate-like structures; prestressed concrete; vibration responses.

**Reference** to this paper should be made as follows: Pathirage, T.S. Chan, T.H.T., Thambiratnam, D.P., Nguyen, A. and Moragaspitiya, H.N.P. (2018) 'Prestress evaluation in prestressed concrete plate-like structures', *Int. J. Lifecycle Performance Engineering*, Vol. 2, Nos. 3/4, pp.127–143.

**Biographical notes:** Thisara S. Pathirage is a PhD Scholar of School of Civil Engineering and Built Environment, Queensland University of Technology, Brisbane, Australia. His research areas include health monitoring of bridges and prestress force identification using vibration-based techniques.

Tommy H.T. Chan is a Full Professor of Civil Engineering in the School of Civil Engineering and Built Environment at QUT. He has been actively involved in carrying out research on bridges. He has published over 300 technical articles and near a quarter of a century of experience in structural health monitoring (SHM) of various significant long span bridges in Hong Kong and the mainland China. He is also a Professional Engineer and Fellow of the Hong Kong Institute of Engineers. He is the Founding Chair and President of the Australian Network of Structural Health Monitoring (ANSHM). Besides SHM, his research interests include bridge engineering, structural dynamics, moving force identification, optical fibre sensors and weigh-in-motion studies.

David P. Thambiratnam has 35 years of international experience gained in Sri Lanka, Canada, Singapore and Australia, which includes about 25 years of academic experience and about seven years of industrial experience. His research areas are bridge dynamics and structural health monitoring, performance of structures under impact, blast and seismic loadings and vibration of slender structures. He has published more than 400 publications in these areas.

Andy Nguyen is a structural testing and monitoring expert at QUT and a core member of QUT Structural Dynamics and Health Monitoring research group. He has been a main developer (between 2011 and 2013) and research coordinator (since 2014) of the long-term full-scale vibration monitoring system of the Brisbane's and QUT's landmark Science and Engineering Centre complex. Besides innovative testing and monitoring solutions, his main research interests include vibration-based damage detection, system identification, advance modelling and model updating, and capacity assessment of civil engineering structures.

H.N.P. Moragaspitiya completed his PhD at the Queensland University of Technology and is currently working as a Structural Manager at Burchills Engineering Solutions. He is also the Principal of K and K Consulting Engineers Pty Ltd.

---

## 1 Introduction

Prestressed concrete (PSC) is being extensively used as an effective material for different structural elements of almost all types of concrete structures for many years. It has gained its popularity as a construction material due to its superior performance and a number of other advantages compared to conventional reinforced concrete. Prestress is usually applied to concrete by the means of external or internal tendons anchored to the concrete member. Internal tendons can be either bonded or unbonded. Depending on the time of prestressing, they can be further classified as pre-tensioned or post-tensioned. Both these methods apply an initial stress (essentially compressive stress) to the concrete to counteract the stresses that develop due to self-weight and working loads. These counteracting initial stresses are the main contributor that characterises the high load-carrying capacity of prestressed elements. Thus, PSC can effectively carry loads with smaller sections and less material (both steel and concrete) compared to reinforced concrete. Residual compression closes any formed crack immediately giving an added advantage of self-healing leading to crack-free, durable structures.

In recent years, unbonded post-tensioning in PSC slabs and decks has become increasingly popular as an efficient method with the development in sheathed strands due to several advantages such as higher flexibility of tendons, corrosion protection, small friction losses and ability to complete without grouting (Aeberhard et al., 1990). Unbonded nature in between end anchorages causes the prestress force to transfer to concrete through anchors only causing it to act as external loads to the structure (Breccolotti et al., 2009; Materazzi et al., 2009). Further, it results in a uniform strain distribution along the tendon (Walsh and Kurama, 2010).

Plate-like elements are a common type of structural form in many structures including floor slabs in buildings and bridge decks amongst others. Unlike beams, different configuration plate-like structures with a wide range of support conditions can lead them to different and complex vibration behaviour. However, a smaller thickness compared to other dimensions characterises and dominates their plate behaviour in vibration analysis. It is clear that this dominant behaviour must be accounted for in an accurate vibration analysis and quantification.

Application of prestressing in plate-like members significantly improves their performance enabling longer spans with thinner sections and less material. Furthermore, prestressing encourages the use of precast plate members leading to speedy construction and cost-effective, high-quality products. As for any other prestressed member, the effective prestress force plays a crucial role in the performance of these structures. Prestress force reduces with time due to prestress losses due to creep and shrinkage of concrete, relaxation of steel etc. and more severely due to defects and damages of the prestressing system. Excessive reduction of effective prestress can lead to poor performance or failure of the structure. Unavailability of a direct measurement method of effective prestress force and impossible visual inspection of tendons are common disadvantages of most prestressed structures which highlight the need for an indirect evaluation method.

Study on prestress force effect and prediction of prestress force has captured the interest of researchers for many years. Methods proposed towards this end by different authors can be broadly categorised into three categories as destructive, semi-destructive and non-destructive methods. Destructive tests usually employ a gradually increasing load till cracking or ultimate failure of the member occurs. Even though several destructive test records (Osborn et al., 2012) show a better estimation of actual capacity and effective prestress force, their applicability is mostly limited to laboratory tests. Semi-destructive tests usually need a small drill hole into the concrete. Stress release at the new free edge created by the drilling is used to calculate the residual stress level. The centre hole stress relief method (Owens, 1993) and concrete core trepanning technique (Kesavan et al., 2005) are some common semi-destructive tests. Amongst these methods, non-destructive test methods in prestress evaluation are becoming increasingly popular over other methods with recent advances in vibration-based structural health monitoring techniques. These methods do not cause any damage to the structure but make use of measurements from externally attached sensors.

Attempts to predict the prestress loss as a damage index by Abraham et al. (1995) is an early stage effort that ended up without success. Since then a number of studies on this topic had come up with some methods to calculate the prestress loss (Kim et al., 2004; Caro et al., 2013) and/or to estimate the effective prestress force (Lu and Law, 2006; Law et al., 2008; Law and Lu, 2005; Wang et al., 2008; Kim et al., 2004) in PSC beams with a reasonable accuracy. Amongst them, the direct inverse method proposed by Law and Lu

(2005) using measured displacement and sensitivity-based finite element model updating method (Lu and Law, 2006), which was also proposed by the same authors identified the prestressed force in prestressed beams with a reasonable accuracy. The wavelet-based method proposed by Law et al. (2008) has a potential to predict the prestress force using measured strain or acceleration response. However, not enough attention has been drawn for prestress force evaluation in plate-like structures using vibration-based methods.

This paper aims to address this gap and proposes an indirect method to estimate the residual effective prestress in unbonded post-tensioned strands of simply supported prestressed plate-like members using their vibration responses. When considering real structures, boundary conditions for plates can vary in a wide range. However, simply supported boundary conditions are quite typical for plate-like structures. Prestressed precast concrete slabs are widely being used in buildings, and they are usually simply supported before completing with a concrete topping (Cement and Concrete Association of Australia, 2003). Further, Birman (2011) discussed some other situations, where the supports of plates can be treated as simply supported.

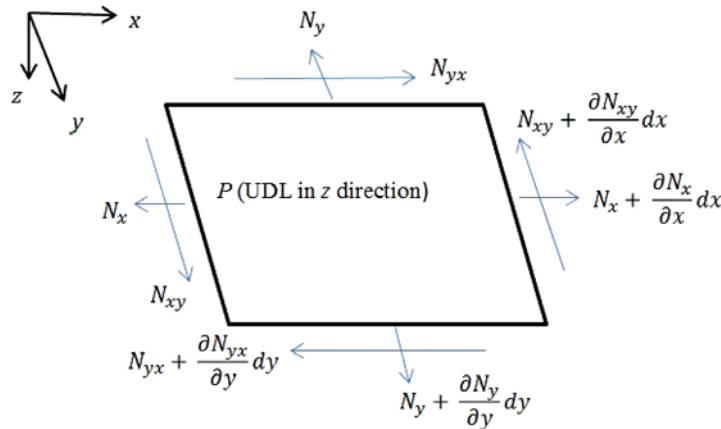
## 2 Vibration of prestressed plates

The use of prestressing encourages longer spanning plate-like members with thinner sections leading to higher span-to-depth ratios with minimum deflections. Lower thickness compared to other dimensions ( $\text{width}/80 < \text{thickness} < \text{width}/8$ ) allows the use of Kirchhoff-Love theory of plates for vibration analysis of these members rather than the Mindlin plate theory which is for thicker plates with a thickness of more than 1/8 times its width (Ventsel and Krauthammer, 2001).

Consider a general plate element as shown in Figure 1. Governing differential equation for mid-surface deflection of a homogeneous isotropic plate can be written as (Timoshenko et al., 1959):

$$D \left[ \frac{\partial^4 w_{(x,y)}}{\partial x^4} + 2 \frac{\partial^4 w_{(x,y)}}{\partial x^2 \partial y^2} + \frac{\partial^4 w_{(x,y)}}{\partial y^4} \right] = P + N_x \frac{\partial^2 w_{(x,y)}}{\partial x^2} + N_y \frac{\partial^2 w_{(x,y)}}{\partial y^2} + 2N_{xy} \frac{\partial^2 w_{(x,y)}}{\partial x \partial y} \quad (1)$$

**Figure 1** Plate element with general loading (see online version for colours)



where  $D = \frac{Eh^3}{12(1-\nu^2)}$  - bending stiffness of the plate,  $w_{(x,y)}$  - displacement of plate in  $z$  direction,  $E$  is modulus of elasticity,  $h$  is plate thickness and  $\nu$  is Poisson's ratio.

$P$  is Applied uniformly distributed load in  $z$  direction

This can be extended to predict the displacement due to a time varying force  $P_{(x,y,t)}$  using D'Alembert's principle as follows:

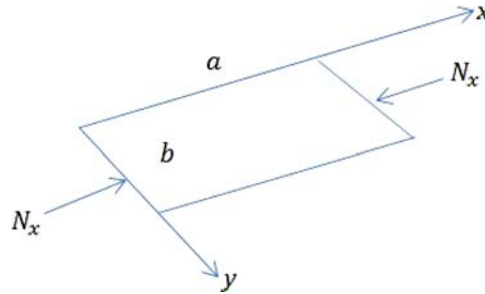
$$D \left[ \frac{\partial^4 w_{(x,y,t)}}{\partial x^4} + 2 \frac{\partial^4 w_{(x,y,t)}}{\partial x^2 \partial y^2} + \frac{\partial^4 w_{(x,y,t)}}{\partial y^4} \right] + C \frac{\partial w_{(x,y,t)}}{\partial t} - N_x \frac{\partial^2 w_{(x,y,t)}}{\partial x^2} - N_y \frac{\partial^2 w_{(x,y,t)}}{\partial y^2} - 2N_{xy} \frac{\partial^2 w_{(x,y,t)}}{\partial x \partial y} = P_{(x,y,t)} - M \frac{\partial^2 w_{(x,y,t)}}{\partial t^2} \quad (2)$$

where  $C$  - damping ratio,  $M$  - mass of plate per unit area,  $t$  - time.

For the case of prestressed plates with prestressing in one direction only, assuming a plate of following configuration with dimensions  $a$  and  $b$  as in Figure 2, Eq. (2) can be further simplified to

$$D \left[ \frac{\partial^4 w_{(x,y,t)}}{\partial x^4} + 2 \frac{\partial^4 w_{(x,y,t)}}{\partial x^2 \partial y^2} + \frac{\partial^4 w_{(x,y,t)}}{\partial y^4} \right] + C \frac{\partial w_{(x,y,t)}}{\partial t} - N_x \frac{\partial^2 w_{(x,y,t)}}{\partial x^2} = P_{(x,y,t)} - M \frac{\partial^2 w_{(x,y,t)}}{\partial t^2} \quad (3)$$

**Figure 2** Plate with prestressing in  $x$  direction only (see online version for colours)



Using modal superposition, the solution to the above equation can be written in the form of

$$w_{(x,y,t)} = \sum_{m=1}^{\infty} \sum_{n=1}^{\infty} \varphi_{m,n}(x,y) W_{m,n}(t) \quad (4)$$

where  $\varphi_{m,n}(x,y)$  is the mode shape function and  $W_{m,n}(t)$  is the modal amplitude.

For a simply supported plate, it can be shown that

$$\varphi_{m,n}(x,y) = \sin\left(\frac{m\pi x}{a}\right) \sin\left(\frac{n\pi y}{b}\right) \quad (5)$$

where  $m, n$  are the number of half sine waves in  $x$  and  $y$  directions, respectively. Further, external excitation force can be expressed as a double Fourier series as,

$$P_{(x,y,t)} = \sum_{m=1}^{\infty} \sum_{n=1}^{\infty} P_{(m,n,t)} \sin\left(\frac{m\pi x}{a}\right) \sin\left(\frac{n\pi y}{b}\right) \quad (6)$$

By substituting Eqs. (4)–(6) in Eq. (3) and simplifying,

$$M \ddot{W}_{m,n(t)} + C \dot{W}_{m,n(t)} + (\alpha^2 + \beta^2)^2 \left[ D - \frac{\alpha^2 N_x}{(\alpha^2 + \beta^2)^2} \right] W_{m,n(t)} = P_{m,n,t} \quad (7)$$

where  $\alpha = \frac{m\pi}{a}$  and  $\beta = \frac{n\pi}{b}$

Comparing Eq. (7) with the general form of equation of motion, the modal stiffness of the simply supported plate with an in-plane load is

$$(\alpha^2 + \beta^2)^2 \left[ D - \frac{\alpha^2 N_x}{(\alpha^2 + \beta^2)^2} \right]$$

$\alpha^2 N_x$  is the reduction in modal bending stiffness due to the in-plane compressive load which is commonly known as compression softening (Saiidi et al., 1994; Materazzi et al., 2009).

### 3 Prestress force estimation from measured vibration responses

#### 3.1 Prestress identification

Equation (4) gives the displacement response  $w_{(x,y,t)}$  at any  $(x, y)$  point.

By taking first and second derivatives with respect to time, velocity and acceleration can be expressed as,

$$\dot{w}_{(x,y,t)} = \sum_{m=1}^{\infty} \sum_{n=1}^{\infty} \phi_{m,n}(x, y) \dot{W}_{m,n}(t) \quad (8a)$$

$$\ddot{w}_{(x,y,t)} = \sum_{m=1}^{\infty} \sum_{n=1}^{\infty} \phi_{m,n}(x, y) \ddot{W}_{m,n}(t) \quad (8b)$$

In matrix form,

$$[w]_{p \times 1} = [\phi]_{p \times q} [W_{(t)}]_{q \times 1} \quad (8c)$$

where  $p$  is the number of measurement locations and  $q$  is the number of modes considered in the calculation. Then the generalised modal coordinate matrix can be obtained from Eq. (8c) as,

$$[W_{(t)}] = ([\phi]^T [\phi])^{-1} [\phi]^T [w] \quad (9a)$$

The matrix inversion  $([\varphi]^T [\varphi])^{-1}$  is found to be highly ill conditioned leading to a large error. In order to bound the solution, Tikhonov regularisation is used as in Eq. (9b).

$$[W_{(t)}] = ([\varphi]^T [\varphi] + [\Gamma])^{-1} [\varphi]^T [w] \quad (9b)$$

where the regularisation term  $\Gamma$  is the Tikhonov matrix selected to minimise

$$\|[\varphi][W_{(t)}] - [w]\|^2 + \|[\Gamma][W_{(t)}]\|^2$$

Similarly,

$$[\dot{W}_{(t)}] = ([\varphi]^T [\varphi] + [\Gamma])^{-1} [\varphi]^T [\dot{w}] \quad (9c)$$

$$[\ddot{W}_{(t)}] = ([\varphi]^T [\varphi] + [\Gamma])^{-1} [\varphi]^T [\ddot{w}] \quad (9d)$$

where  $w$ ,  $\dot{w}$  and  $\ddot{w}$  are the measured displacement, velocity and acceleration responses, respectively.

For an excitation force of  $P_{of(t)}$ ,

$$P_{m,n,t} = P_{(m,n)} f_{(t)}$$

$$\text{where } P_{(m,n)} = \frac{4}{ab} \int_0^a \int_0^b P_{(x,y)} \sin(\alpha x) \sin(\beta y) dx dy \quad (10)$$

It can be shown that, for a point load at  $(\xi, \eta)$

$$P_{(m,n)} = \frac{4P_0}{ab} \sin(\alpha\xi) \sin(\beta\eta) \quad (11)$$

Equation (7) can be written in matrix form as,

$$M[\ddot{W}_{(t)}] + [C][\dot{W}_{(t)}] + [D_0 - \alpha^2 N_x][W_{(t)}] = [P_t] \quad (12)$$

where  $[D_0] = \text{diag}((\alpha^2 + \beta^2)^2 D)$ . Then,

$$[\alpha^2 N_x][W_{(t)}] = M[\ddot{W}_{(t)}] + [C][\dot{W}_{(t)}] + [D_0][W_{(t)}] - [P_t] \quad (13)$$

This is in the form,

$$[X]N_x = [A]$$

where  $[X] = [\alpha^2][W_{(t)}]$  and  $[A]$  is the RHS of Eq. (13).

Then,  $N_x$  can be obtained from damped least square inversion as,

$$N_x = ([X]^T [X] + \lambda [I])^{-1} [X]^T [A] \quad (14)$$

where  $\lambda$  is the non-negative damping coefficient and  $[I]$  is the identity matrix.

### 3.2 Numerical simulation

A simply supported plate of  $3\text{ m} \times 6\text{ m} \times 0.2\text{ m}$  was used to verify the above method and study the effect of the presence of an axial force on vibration. The plate was modelled using shell elements and a uniform in-plane compressive force was applied to simulate the prestress effect. Properties of the plate were selected as  $E = 30\text{ GPa}$ ,  $\nu = 0.2$  and the mass density of concrete as  $2400\text{ kg/m}^3$  which gives a mass per unit area of  $M = 480\text{ kg/m}^2$ . A modal analysis was carried out to evaluate the effect of prestressing on the natural frequency of vibration. First six vibration modes and corresponding  $m, n$  values are shown in Figure 3. Variation of modal frequencies with the axial force is as shown in Table 1.

**Figure 3** First six mode shapes (see online version for colours)

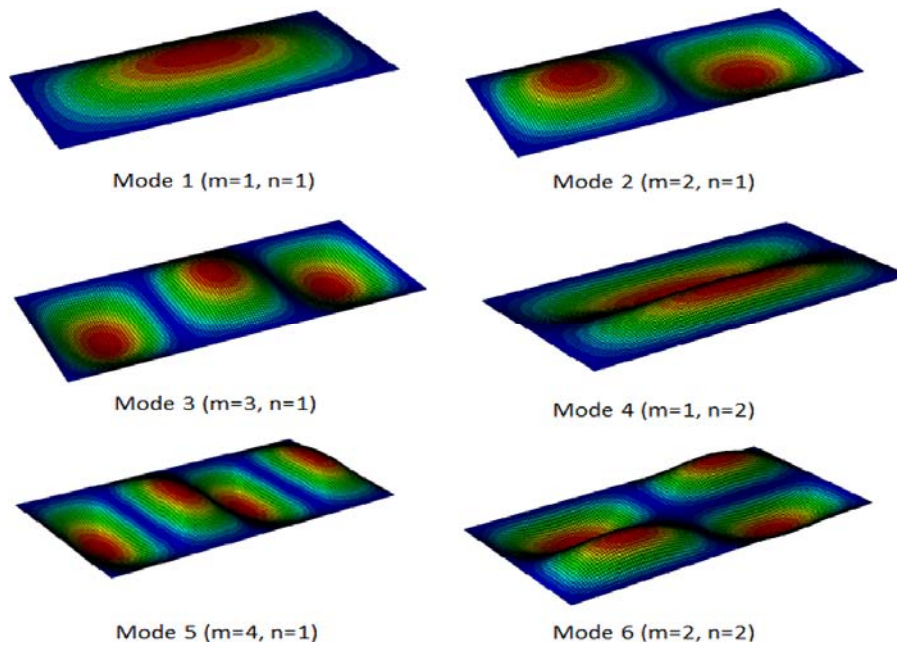


**Table 1** Effect of prestress force on modal frequencies

Mode		Frequency (Hz)			
$m$	$n$	$N_x = 0$	$N_x = 1 \times 10^6$	$N_x = 2 \times 10^6$	$N_x = 4 \times 10^6$
1	1	45.45	45.29	45.13	44.81
2	1	72.72	72.32	71.92	71.11
3	1	118.17	117.62	117.07	115.94
1	2	154.53	154.48	154.44	154.34
4	1	181.81	181.16	180.53	179.24
2	2	181.90	181.64	181.47	181.15

### 3.3 Prestress force identification

The same plate was excited using a sinusoidal periodic excitation force of  $5000 \sin(15\pi t)$  N at  $P = (2, 1.5)$  to extract the vibration responses for prestress force identification. Damping of the plate was considered as 2% for all modes. The coordinates shown in the brackets are in meters. For demonstration purposes, vibration responses were recorded at two sensor locations as  $S1 = (1.5, 2.25)$  and  $S2 = (4.5, 0.75)$  as shown in Figure 4. Effect of sensor locations and the number of sensors will be discussed in Section 3.5 of this paper. Excitation location was selected randomly. There is no specific requirement in selecting this point. However, it is recommended to choose a point towards the middle of the plate to obtain higher quality response data (i.e. data with a better signal-to-noise ratio). Measured displacement and acceleration responses at two sensor locations of the prestressed and unprestressed plate are given in Figure 5. Data were recorded at a sampling rate of 1000 Hz.

**Figure 4** Excitation (P) and sensor (S1 and S2) locations

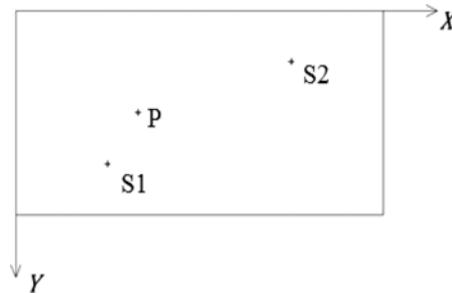
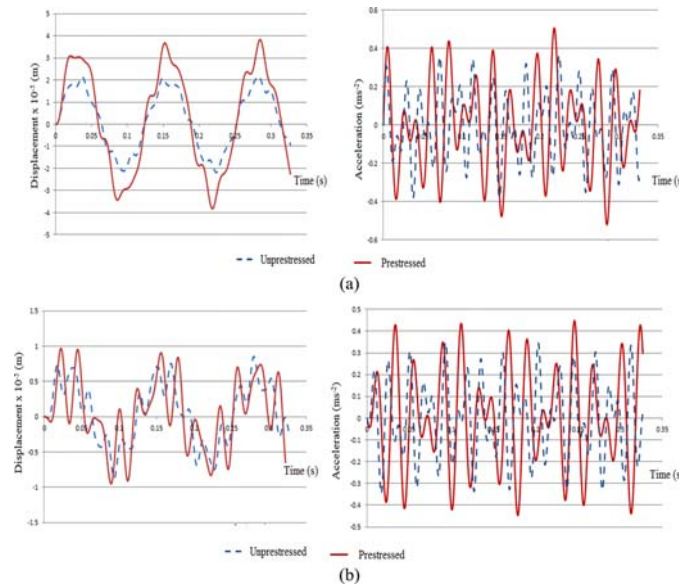


**Figure 5** Measured displacement and acceleration responses at (a) S1 and (b) S2 (see online version for colours)



It is found that a minimum of six modes must be considered for the convergence of the double Fourier series which has been employed in Eq. (6) to approximate the excitation force. Hence the first six modes were used in the inverse calculation to estimate the prestress force.

In practical applications, vibration data always get polluted with measurement noise and accuracy of the result can be affected. In order to study the effect of noise, a white noise was added to both signals as;

$$w_{(\text{noisy})} = w_{(\text{calculated})} + \text{noise}$$

$$\dot{w}_{(\text{noisy})} = \dot{w}_{(\text{calculated})} + \text{noise}$$

The noise was calculated as;

$$\text{noise} = N_L \times r \times \text{rms}(R)$$

where  $N_L$  is the noise level,  $r$  is a random number drawn from standard normal distribution with a zero mean and unit standard deviation and  $\text{rms}(R)$  is the root mean square value of measured response. Examples of identified forces with and without noise are shown in Figure 6. The use of random number ( $r$ ) in the noise model generates different noise patterns for a selected noise level at every calculation attempt leading to slightly varied percentage errors. For the purpose of error quantification, calculation has been repeated a number of times (100) and the maximum error was taken as the upper bound of the error due to measurement noise. Average of identified forces as per Figure 7, percentage errors with maximum error, average and standard deviation of percentage errors are shown in Table 2. The average error of identification with 10% noise is very close to the error of without noise identification. Standard deviation of percentage error of 100 calculations is also very small. This shows that the proposed method is robust against noisy measurements.

**Figure 6** Effect of measurement noise on identification (see online version for colours)

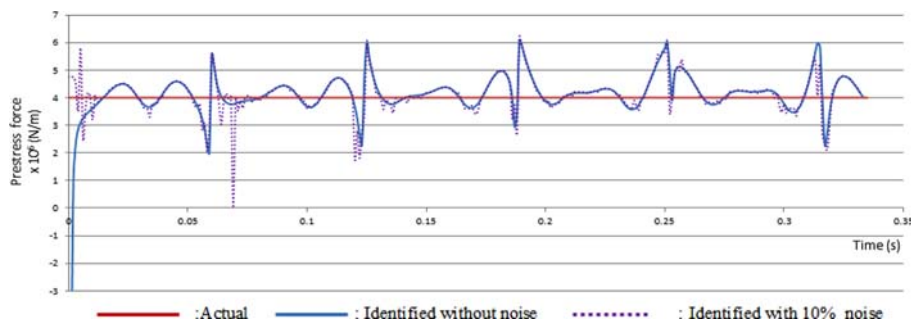


**Figure 7** Identified prestress forces with a periodic excitation (see online version for colours)

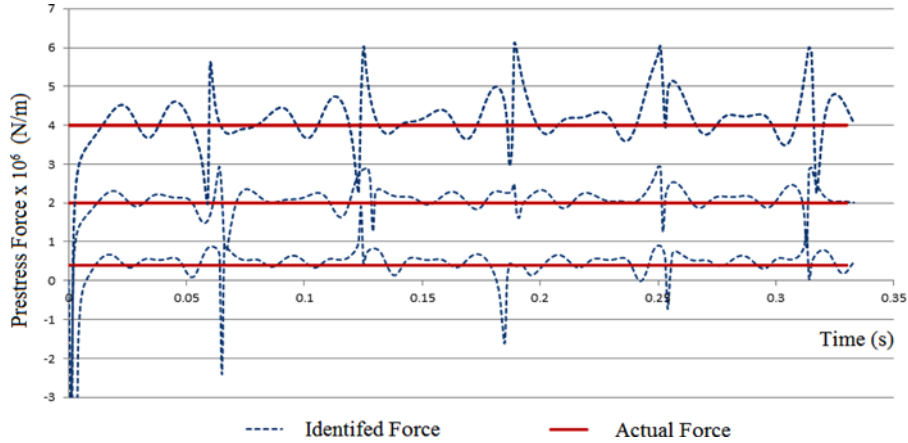


**Table 2** Identified average prestress forces and percentage errors (%)

Actual prestress force (N/m)	Average prestress force (N/m)	
	Without noise (error)	With 10% noise (max error, average error, standard deviation)
$4.0 \times 10^6$	$4.171 \times 10^6$ (4.27%)	$4.273 \times 10^6$ (6.83, 5.21, 0.71%)
$2.0 \times 10^6$	$2.194 \times 10^6$ (9.69%)	$2.235 \times 10^6$ (11.75, 10.19, 0.66%)
$0.4 \times 10^6$	$0.442 \times 10^6$ (10.51%)	$0.452 \times 10^6$ (13.02, 11.53, 0.81%)

### 3.4 Optimum use of sensors

Effect of number of sensors and the position of these sensors on the accuracy of prediction were studied to optimise the sensor usage. Arbitrarily distributed six sensor locations were selected to extract responses as shown in Figure 8.

**Figure 8** Sensor locations



A parametric study carried out reveals that measurements from two measurement locations can predict the prestress force with a good accuracy. Time histories of identified forces with different sensor combinations are shown in Figure 9. As presented in Figure 10 and Table 3, use of more measurements may improve the accuracy of identified value but the improvement is fairly marginal in relation to the number of sensors. On the other hand, the use of only one measurement point should be avoided,

since this will give comparatively high variation. It is also found that the sensor location can have some effect on the identified results as shown in Figure 11. Higher amplitude responses from sensors close to the excitation point such as S1 and S3 in Figure 8 result in better identification accuracy than those from other sensor locations such as S2 and S4.

**Figure 9** Effect of number of sensor locations on prestress identification (see online version for colours)

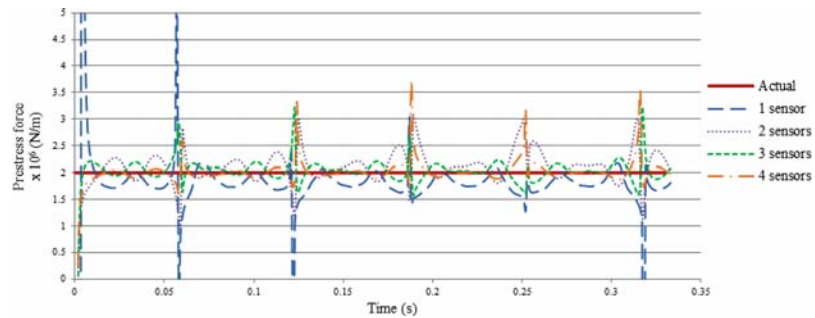


**Figure 10** Change in percentage error with number of sensors (see online version for colours)

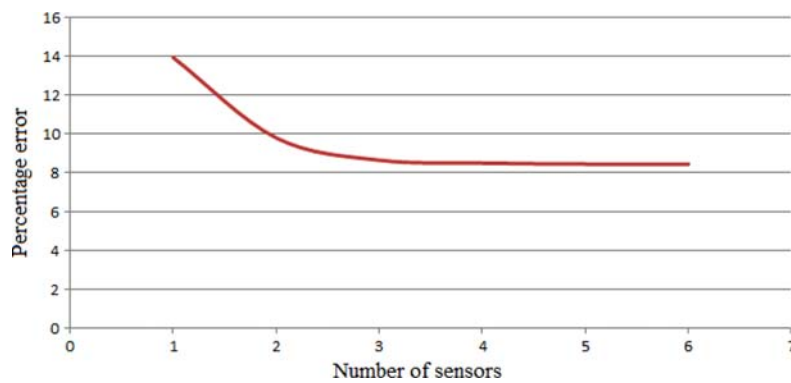


**Figure 11** Effect of sensor location on prestress force identification (see online version for colours)

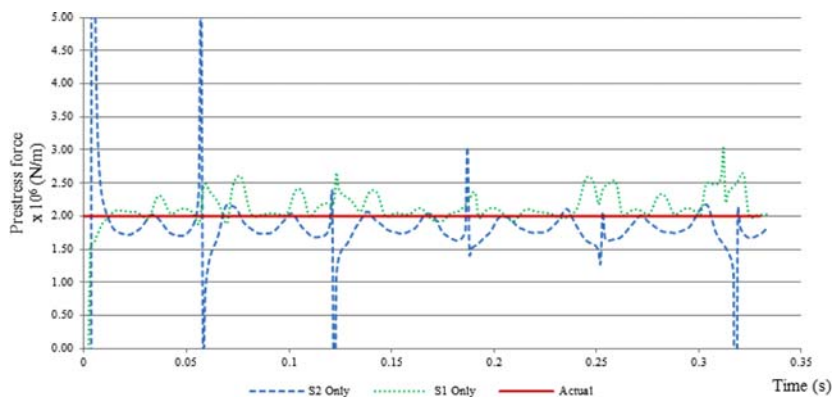


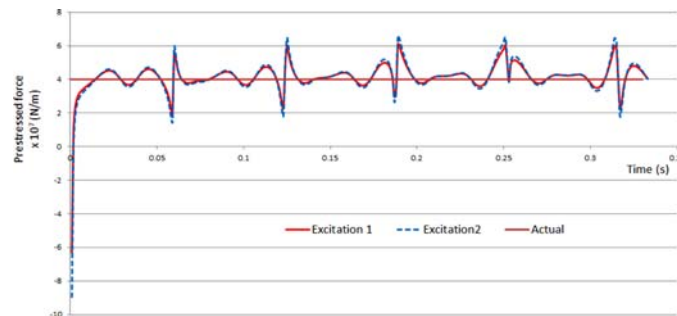
**Table 3** Identified average prestress forces and percentage errors (%) - effect of number of sensor locations

<i>Number of sensor locations</i>	<i>Average prestress force, N/m (error)</i>
1	$1.721 \times 10^6$ (13.95%)
2	$2.196 \times 10^6$ (9.80%)
3	$2.176 \times 10^6$ (8.65%)
4	$2.170 \times 10^6$ (8.50%)
5	$2.169 \times 10^6$ (8.45%)
6	$2.169 \times 10^6$ (8.45%)

### 3.5 Effect of excitation force

Figure 12 shows the identified force for two different excitation magnitudes. Excitation 1 is the same excitation force used in above study and the excitation 2 is 20% higher in magnitude. No significant effect of magnitude of the excitation force on identified results was observed. However, the magnitude of vibration responses varies with the level of excitation. Consequently, for practical situations, the level of excitation may have to be selected depending on the sensitivity and measurable range of sensors.

**Figure 12** Effect of excitation force magnitude (see online version for colours)



### 3.6 Effect of damping

Damping ratio of the structure can vary from structure to structure depending on the material properties and geometric variations. Identified prestress force in the proposed method showed a minor variation for the damping ratio as shown in Table 4.

**Table 4** Effect of damping

<i>Actual prestress force (N/m)</i>	<i>Average prestress force, N/m (error)</i>	
	<i>Without damping</i>	<i>With 2% damping</i>
$4.0 \times 10^6$	$4.164 \times 10^6$ (4.1%)	$4.171 \times 10^6$ (4.27%)
$2.0 \times 10^6$	$2.191 \times 10^6$ (9.55%)	$2.194 \times 10^6$ (9.69%)
$0.4 \times 10^6$	$0.441 \times 10^6$ (10.25%)	$0.442 \times 10^6$ (10.51%)

### 3.7 Identification from impulsive excitation

The above method was further verified using an impulsive excitation of magnitude 6000 N as shown in Figure 13. Use of impulsive excitation is more beneficial than a periodic excitation in terms of practicality. An impulse load can be applied easily by means of drop weight than applying a periodic force which needs special heavy machineries. Effective prestress force can be calculated with a good accuracy using measurements from two locations as shown in Figure 14. Neglecting the initial estimations with high magnitude due to initial impact of excitation, the average identified force is  $1.91 \times 10^6$  N/m which has an error of as low as 4.5%.

**Figure 13** Impulsive excitation (see online version for colours)

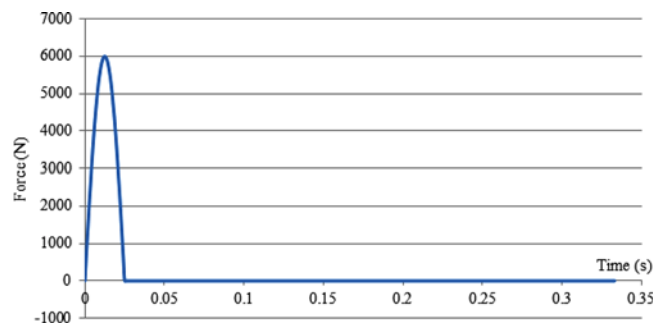
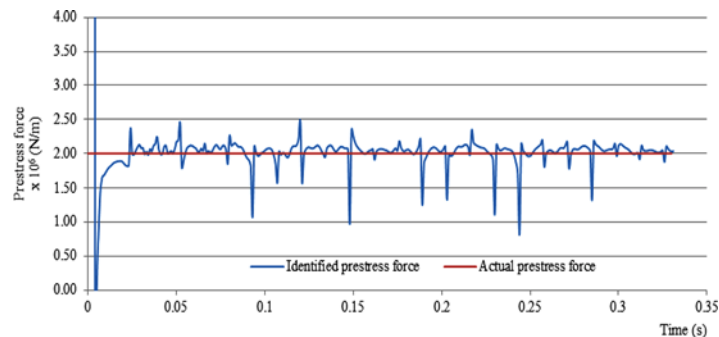


**Figure 14** Identified prestress force using impulsive excitation (see online version for colours)

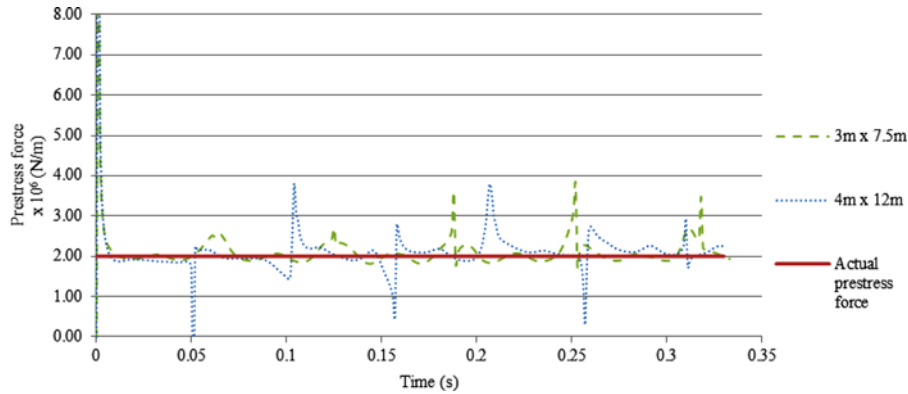


### 3.8 Applicability to different plate sizes

The size of these plate structures can vary depending on the application. Long span prestressed floors are a common application. According to guideline of Cement and Concrete Association Australia (1988), prestressed single span flat plates are being commonly used for floors having a span of 6–12 m with the most economical range of 6–10 m. In order to assess the validity of the proposed method to plates with longer spans in the practical range, two other plates of dimensions 3 m  $\times$  7.5 m and 4 m  $\times$  12 m were studied. Three plates that were studied cover possible short (6 m), medium (7.5 m) and long (12 m) span plates with span/width ratio of 2, 2.5 and 3, respectively. Time histories of identified prestress forces from periodic excitations are shown in Figure 15. Identified

forces are of good accuracy with error in identification as less as 7.48% for the first plate and 7.35% for the second plate. Hence the proposed method does not depend on the size of plate and applicable to a practical range of prestressed plates.

**Figure 15** Identified prestress force for different plate sizes (see online version for colours)



#### 4 Discussion and conclusion

Prestressed plate-like members are a common form of PSC structures. Smaller height compared to other dimensions distinguishes their dominating plate action. As with any other prestressed member, the effective prestress force plays a pivotal role on their performance. The literature does not report any method to assess the effective prestress force in these types of members using vibration-based methods. This paper presents a new approach to estimate the effective prestress force in unbonded post-tensioned tendons in simply supported plate-like structures which have not been studied before. Displacement and acceleration responses due to a periodic and impulsive excitation were used in the analysis.

It is observed that in-plane compressive force reduces the natural frequency due to well-known compression softening effect. The proposed method can accurately estimate the effective prestress force using data collected at two locations only. Use of more sensor points improves the results marginally, whereas use of only one sensor point only should be avoided due to the higher deviation of results from the actual value. The average value of identified prestress force matches the actual force with good accuracy. When the structure is excited using a periodic load, the maximum error of identified force without noise is 10.51% and with the noise it is 13.02% for the common range of prestresses. Hence the proposed method is robust for noisy measurements. It should be noted that even though the identification error increases with lower prestress forces, the trend rapidly converges when approaching the common prestress range which is 1–5 MPa (Khan and Williams, 1995; Aeberhard et al., 1990).

A higher variation in prestress force estimates was observed at some points as in Figures 6 and 7. These points are related to the point of change in direction of displacement response around which the displacement becomes very small. As a result, close to this point  $[W_{(t)}]$  in Eq. (9a) becomes very small which gives a very high value

for the inversion  $([X])^{-1}$ . Further, change in direction of displacement from positive to negative changes the direction of convergence of results. However, use of damped least square inversion as in Eq. (14) significantly reduces this effect.

Proposed method requires a measured external excitation force for the identification process. Use of measured force vibration in structural testing is common and has been used with a number of structures in the past (Armer, 2001; Farrar et al., 1999). Further, the ability to use an impulsive excitation force as proposed in this paper adds more practical value to the proposed method as the impact excitation is much easier to apply and measure using instrumented impulse hammers than shaker excitation which require heavy machines (Reynolds and Pavic, 2000). However, for real applications, impact excitation is more suitable for small structures, whilst shaker excitation is better for larger structures. Future works will focus on further reducing the identification error with more rigorous regulation techniques and validating the proposed method as well as related excitation schemes through experiments.

## References

- Abraham, M.A., Park, S. and Stubbs, N. (1995) 'Loss of prestress prediction based on nondestructive damage location algorithms', *Smart Structures & Materials* '95, 26/02/1995 1995 San Diego, California, International Society for Optics and Photonics, pp.60–67.
- Aeberhard, H., Ganz, H., Marti, P. and Schuler, W. (1990) *Post-tensioned Concrete in Building Construction - Post-Tensioned Foundations*. Switzerland: VSL- International LTD.
- Armer, G.S.T. (2001) *Monitoring and Assessment of Structures*, Spon Press, Florence, New York (Imprint).
- Birman, V. (2011) *Plate Structures*, Springer, Dordrecht.
- Brecolotti, M., Ubertini, F. and Venanzi, I. (2009) 'Natural frequencies of prestressed concrete beams: theoretical prediction and numerical validation', *Atti del del XIX Congresso AIMETA*, September 2009 Italy, pp.14–17.
- Caro, L.A., Marti-vargas, J.R. and Serna, P. (2013) 'Prestress losses evaluation in prestressed concrete prismatic specimens', *Engineering Structures*, Vol. 48, pp.704–715.
- Cement and Concrete Association of Australia (1988) *Design Guide for Long-span Concrete Floors*, Cement and Concrete Association of Australia in Collaboration with Steel Reinforcement Promotion Group, North Sydney.
- Cement and Concrete Association of Australia (2003) *Guide to Long Span Concrete Floors*, Cement and Concrete Association of Australia, St Leonards, NSW.
- Farrar, C.R., Duffey, T., Cornwell, P.J. and Doebling, S.W. (1999) 'Excitation methods for bridge structures', *Society for Experimental Mechanics, Inc., 17th International Modal Analysis Conference*, February 1999 Florida, pp.1063–1068.
- Kesavan, K., Ravisankar, K., Parivallal, S. and Sreeshylam, P. (2005) 'Technique to assess the residual prestress in prestressed concrete members', *Experimental Techniques*, Vol. 29, pp.33–38.
- Khan, S. and Williams, M. (1995) *Post-tensioned Concrete Floors*, Great Britain, CRC press.
- Kim, J-T., Yun, C-B., Ryu, Y-S. and Cho, H-M. (2004) 'Identification of prestress-loss in PSC beams using modal information', *Structural Engineering and Mechanics*, Vol. 17, pp.467–482.
- Law, S.S. and Lu, Z.R. (2005) 'Time domain responses of a prestressed beam and prestress identification', *Journal of Sound and Vibration*, Vol. 288, pp.1011–1025.

- Law, S.S., Wu, S.Q. and Shi, Z.Y. (2008) 'Moving load and prestress identification using wavelet-based method', *Journal of Applied Mechanics*, Vol. 75, pp.021014–021014.
- Lu, Z.R. and Law, S.S. (2006) 'Identification of prestress force from measured structural responses', *Mechanical Systems and Signal Processing*, Vol. 20, pp.2186–2199.
- Materazzi, A., Breccolotti, M., Ubertini, F. and Venanzi, I. (2009) 'Experimental modal analysis for assessing prestress forces in PC bridges: a sensitivity study', *Proc. III International Operational Modal Analysis Conference*, 4-6 May 2009 Portonovo, Italy, pp.4–6.
- Osborn, G., Barr, P., Petty, D., Halling, M. and Brackus, T. (2012) 'Residual prestress forces and shear capacity of salvaged prestressed concrete bridge girders', *Journal of Bridge Engineering*, Vol. 17, pp.302–309.
- Owens, A. (1993) 'In-situ stress determination used in structural assessment of concrete structures', *Strain*, Vol. 29, pp.115–124.
- Reynolds, P. and Pavic, A. (2000) 'Impulse hammer versus shaker excitation for the modal testing of building floors', *Experimental Techniques*, Vol. 24, pp.39–44.
- Saiidi, M., Douglas, B. and Feng, S. (1994) 'Prestress force effect on vibration frequency of concrete bridges', *Journal of structural Engineering*, Vol. 120, pp.2233–2241.
- Timoshenko, S., Woinowsky-Krieger, S. and Woinowsky-Krieger, S. (1959) *Theory of Plates and Shells*, McGraw-Hill, New York.
- Ventsel, E. and Krauthammer, T. (2001) *Thin Plates and Shells: Theory, Analysis, and Applications*, New York, Marcel Dekker Inc.
- Walsh, K.Q. and Kurama, Y.C. (2010) 'Behavior of unbonded posttensioning monostrand anchorage systems under monotonic tensile loading', *PCI Journal*, Vol. 55, pp.97–117.
- Wang, Y., Zhu, X-Q., Hao, H. and Ou, J-P. (2008) 'Identification of prestress force in concrete beams by finite element model updating', *International Symposium on Structural Engineering for Young Experts*, Oct 2008, Changsha, China: Science press.